An Electrically Switchable Optical Ultrawideband Pulse Generator

Qing Wang and Jianping Yao, *Senior Member, IEEE, Member, OSA*

***Abstract*—A novel electrically switchable optical ultrawideband (UWB) pulse generator that is capable of generating both Gaussian monocycle and Gaussian doublet pulses by using a polarization modulator (PolM) and a fiber Bragg grating is proposed and experimentally demonstrated. The polarity and the shape of the generated UWB pulses can be electrically switched by adjusting the voltages applied to two arbitrary wave plates (AWPs), which are incorporated at the input and the output of the PolM to adjust the polarization state of the lightwaves. The key component in the UWB pulse generator is the PolM, which is a special phase modulator that can support both transverse electric and transverse magnetic modes but with opposite phase modulation indexes. Depending on the polarization state of the incident lightwave to the PolM that is linearly polarized and aligned to one principle axis of the PolM or circularly polarized, UWB monocycle or doublet pulses are generated. The polarity of the UWB pulses can be electrically switched by adjusting the voltages applied to the AWPs. The proposed system is implemented, and the generation of UWB monocycle and doublet pulses is experimentally demonstrated. Gaussian monocycle and doublet pulses with a fractional bandwidth of about 150% and 160% are experimentally generated. The proposed electrically switchable optical UWB pulse generator has the potential for applications in UWB communications and radar systems that employ pulse polarity modulation and pulse shape modulation schemes.**

***Index Terms*—Frequency discrimination, Gaussian doublet, Gaussian monocycle, phase modulation (PM), polarization modulator (PolM), switchability, ultrawideband (UWB).**

I. Introduction

ULTRAWIDEBAND (UWB) is considered to be a promising technology for short-range high-data-rate wireless communication systems and sensor networks due to the many advantageous features such as low power consumption, low spectral density, high immunity to multipath fading, enhanced capability to penetrate through obstacles, and coexistence with other conventional radio systems [1]–[5]. In 2002, the U.S. Federal Communications Commission (FCC) approved the unlicensed use of the UWB spectrum from 3.1 to 10.6 GHz for indoor communications, with a power spectral density (PSD) lower than -41.3 dBm/MHz [1]. Based on the FCC definition, a UWB signal should have a spectral bandwidth greater than 500 MHz or a fractional bandwidth greater than 20% [1].

Manuscript received June 20, 2007; revised August 11, 2007. This work was supported by the Natural Sciences and Engineering Research Council of Canada (NSERC).

The authors are with the Microwave Photonics Research Laboratory, School of Information Technology and Engineering, University of Ottawa, Ottawa, ON K1N 6N5, Canada (e-mail: jpyao@site.uOttawa.ca).

Color versions of one or more of the figures in this paper are available online at http://ieeexplore.ieee.org.

Digital Object Identifier 10.1109/JLT.2007.907749

For UWB communications, one of the many challenges is to generate UWB pulses that have a power spectrum meeting the FCC-specified spectral mask. Different UWB pulse generation techniques have been recently proposed [6]–[16]. Among these techniques, the implementation of the first- or the second-order derivatives of a Gaussian pulse, to generate a Gaussian monocycle or a Gaussian doublet, is considered a simple and efficient technique for the UWB pulse generation [4]. The UWB pulses can be directly generated in the electrical domain by using a high-speed electrical circuitry such as an electrical frequency differentiator [6]–[9]. Recently, the generation of electrical UWB pulses in the optical domain has attracted great interest. Compared to the electrical techniques using electrical circuitry, the generation of the UWB signals in the optical domain provides a higher flexibility, which enables the generation of the UWB pulses with different shapes and switchable polarity. In addition, the huge bandwidth offered by optics enables the generation of the UWB pulses to fully occupy the spectrum range specified by the FCC. These optical approaches include the generation of the UWB pulses using a frequency-shift-keying modulator [10], a nonlinearly biased Mach–Zehnder modulator [11], a two-tap microwave delay-line filter with coefficients of $(1\ -1)$ [12], or an optical spectrum shaper with frequency-to-time mapping [13], [14]. Very recently, the UWB pulse generation based on electrooptic phase modulation (PM) and PM to intensity modulation (IM) conversion has been demonstrated [15], [16]. The PM–IM conversion is implemented using either a frequency discriminator [15] or chromatic dispersive element [16]. Gaussian monocycle or doublet pulses were generated by the PM–IM conversion. In [15], with a single fiber Bragg grating (FBG) serving as a frequency discriminator, either a UWB monocycle or doublet was generated by locating the optical carrier at the linear or the quadrature region of the FBG reflection spectrum. By simply switching the wavelength of the optical carrier between the linear and the quadrature regions, the shape of the UWB pulses was switched between a monocycle and a doublet. The polarity of the pulses can also be switched by locating the wavelength of the optical carrier between the opposite slopes of the FBG. Therefore, the approach in [15] can be used to implement two important modulation schemes—pulse polarity modulation (PPM) and pulse shape modulation (PSM). A major limitation of the approach in [15] is the limited speed of wavelength switching, which may not be suitable for a UWB communication system operating at a high data rate. In a UWB communication system, to implement the PPM or PSM, it is highly desirable that the UWB pulses can be switched at a speed higher than 100 MHz [4].

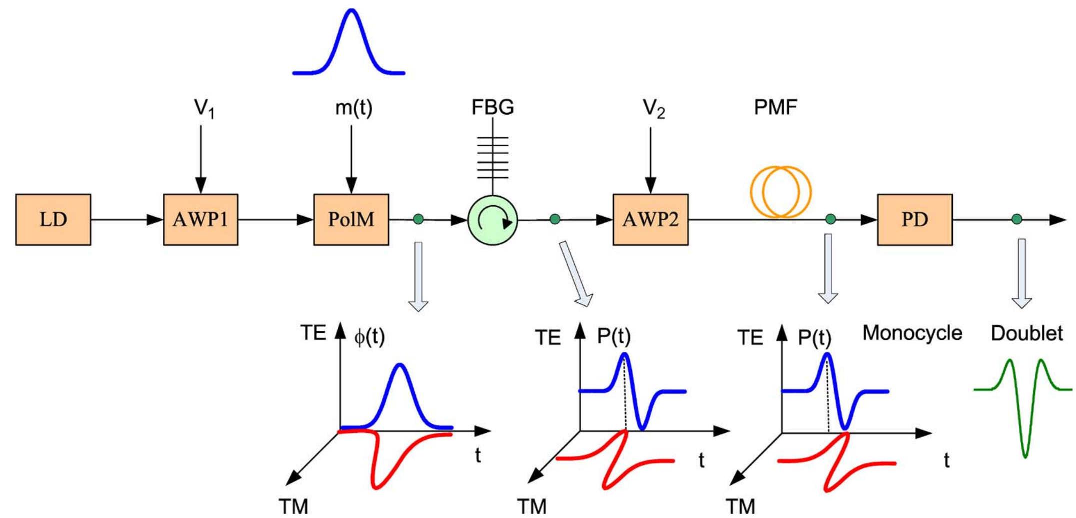

Fig. 1. Schematic of the electrically switchable UWB pulse generator. LD: Laser diode. AWP: Arbitrary wave plate. PolM: Polarization modulator. FBG: Fiber Bragg grating. PMF: Polarization Maintaining fiber. PD: Photodetector.

In this paper, we propose a novel electrically switchable UWB pulse generator that is capable of generating both Gaussian monocycle and Gaussian doublet pulses at a high speed by using a polarization modulator (PolM) and an FBG. The polarity and shape of the UWB pulses can be switched by controlling the voltages applied to two electrically tunable arbitrary wave plates (AWPs). The key component in the system is the PolM, which is a special phase modulator that can support both transverse electric (TE) and transverse magnetic (TM) modes but with opposite PM indexes. Depending on the polarization state of the incident lightwave to the PolM, a UWB monocycle or doublet is generated. Specifically, to generate a UWB monocycle, the incident lightwave to the PolM should be linearly polarized and aligned to one principle axis of the PolM. To generate a UWB doublet, the incident lightwave should be circularly polarized. The polarization state of the incident lightwave is controlled by adjusting the voltage applied to the input AWP. In addition, the polarity of the pulses can also be electrically switched by adjusting the voltages applied to the AWPs. To switch the polarity of a UWB monocycle, we should rotate the polarization direction of the lightwave incident to the PolM by 90°, which was realized by adjusting the voltage applied to the input AWP. To switch the polarity of a UWB doublet, we should rotate the TE and TM modes exiting from the PolM by 90°, which was realized by adjusting the voltage applied to the output AWP. The proposed system is implemented, and the generation of the UWB monocycles and doublets is experimentally demonstrated. Gaussian monocycle and doublet pulses with a fractional bandwidth of about 150% and 160% are experimentally generated. This electrically switchable optical UWB pulse generator has the potential for applications in the UWB communications systems employing PPM and PSM schemes.

II. Principle

A. System Architecture

The schematic of the proposed electrically switchable UWB pulse generator is shown in Fig. 1. The system consists of a laser diode (LD), a PolM, two electrically tunable AWPs, a length of polarization maintaining fiber (PMF), an FBG, and a photodetector (PD). The key component in the system is the PolM, which is a special phase modulator [17]. Differing from a commonly used $LiNbO_3$ waveguide phase modulator in which only one polarization mode is supported while the orthogonal polarization mode is highly attenuated, a PolM supports both TE and TM modes but with opposite PM indexes. When an electrical modulation signal is applied to the PolM, the TE and TM polarization modes would experience opposite phase shifts. If an incident lightwave is oriented with an angle of $\pm 45^\circ$ to one principal axis of the PolM, the polarization state of the output lightwave would vary from horizontal to circular and then to vertical as the modulation voltage is varied by a half-wave voltage V_π; thus, polarization modulation is achieved.

The system shown in Fig. 1 can be used to generate UWB monocycle or doublet pulses. To generate a UWB monocycle pulse, the polarization direction of the incident lightwave to the PolM, which was generated from an LD, is aligned with one principal axis of the PolM, e.g., the TE direction, by applying a voltage V_1 to AWP_1. Since the lightwave is traveling only along one principal axis, the PolM is operating as a regular phase modulator with a PM index $\beta_{PM}(TE)$. The phase-modulated lightwave is then sent to an FBG that is connected via a three-port optical circulator. Therefore, the FBG is operating as a reflection filter. When the optical carrier is located at the linear slope of the FBG reflection spectrum, the FBG is operating as a linear frequency discriminator with the phase-modulated signal being converted to an intensity-modulated signal. Mathematically, the output signal after the PM–IM conversion in a linear frequency discriminator is the first-order derivative of the input modulation signal [15]. If the modulation signal is a Gaussian pulse, a Gaussian monocycle pulse is generated. In Section II-B, a detailed theoretical analysis on PM–IM conversion and its application in the UWB monocycle generation will be presented. We will also show that when the incident lightwave is aligned with the orthogonal principal axis, due to the opposite PM index along the orthogonal principal axis, a UWB monocycle that has an inverted polarity is generated.

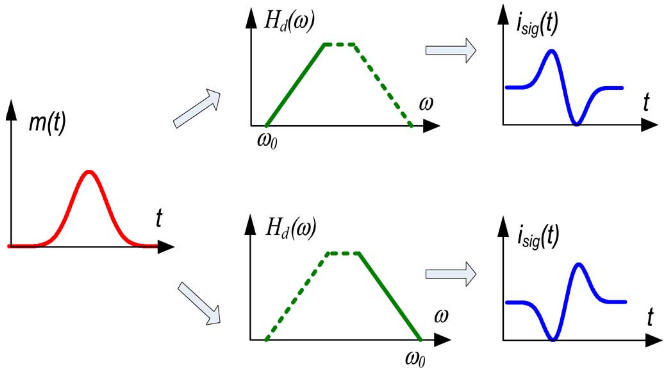

Fig. 2. UWB monocycle generation based on PM-to-IM conversion using an FBG-based frequency discriminator.

The system shown in Fig. 1 can also be used to generate a Gaussian doublet. It is known that a Gaussian doublet is the second-order derivative of a Gaussian pulse or the first-order derivative of the Gaussian monocycle. The operation of a first-order derivative can be approximated by a first-order difference, which can be realized by a two-tap microwave delay-line filter with coefficients of (1 −1) [18]. To achieve this, the polarization state of the lightwave to the PolM is adjusted to be circularly polarized so that the input lightwave is equally projected to the TE and TM directions of the PolM. After PM at the PolM and PM–IM conversion at the FBG, two polarity-inverted monocycles along the TE and TM directions would be generated. By using a second electrically tunable AWP, i.e., AWP_2, to align the TE and TM modes with the fast and slow axes of a length of PMF, two time-delayed monocycles with a time-delay difference determined by the birefringence and the length of the PMF are obtained. A Gaussian doublet that is the superposition of the two time-delayed monocycles is generated at the PD.

B. UWB Monocycle Generation Based on PM–IM Conversions

The normalized optical field of a phase-modulated lightwave can be expressed as

$$E(t) = \exp\left[j\omega_c t + j\beta_{\mathrm{PM}} m(t)\right] \tag{1}$$

where $m(t)$ is the electrical modulation signal applied to the PolM, β_{PM} is the PM index, and ω_c is the angular frequency of the optical carrier. When the optical carrier of the phase-modulated signal is located at the linear slope of the optical bandpass filter, the optical filter is operating as a linear frequency discriminator. A linear PM–IM conversion is thus realized. As shown in Fig. 2, the frequency response of a linear frequency discriminator is given by

$$H_d(\omega) = K(\omega - \omega_0) \tag{2}$$

where K denotes the slope of the frequency response, and ω_0 is the angular frequency that satisfies $H_d(\omega_0) = 0$. When the phase-modulated lightwave is sent to the linear frequency discriminator, the output signal is given by

$$E_{\mathrm{out}}(\omega) = K(\omega - \omega_0)E(\omega) \tag{3}$$

where $E(\omega)$ is the Fourier transform of $E(t)$. Applying the inverse Fourier transform to (3), we have

$$E_{\mathrm{out}}(t) = \left[K(\omega_c - \omega_0) + K\beta_{\mathrm{PM}}\frac{dm(t)}{dt}\right]E(t). \tag{4}$$

Then, the output signal is sent to the PD. After the square-law detection at the PD, the obtained photocurrent is

$$\begin{aligned} i_{\mathrm{PD}}(t) &= \Re\left|E_{\mathrm{out}}(t)\right|^2 \\ &= \Re\left\{K^2(\omega_c - \omega_0)^2 + K^2\beta_{\mathrm{PM}}^2\left[\frac{dm(t)}{dt}\right]^2 \right. \\ &\qquad \left. + 2K^2(\omega_c - \omega_0)\beta_{\mathrm{PM}}\frac{dm(t)}{dt}\right\} \end{aligned} \tag{5}$$

where $\Re$ is the responsivity of the PD. The term $K^2(\omega_c - \omega_0)^2$ in (5) is a dc component. Usually, for a small PM index, $2K^2(\omega_c - \omega_0)\beta_{\mathrm{PM}}(dm(t)/dt) \gg K^2\beta_{\mathrm{PM}}^2[dm(t)/dt]^2$, the term $K^2\beta_{\mathrm{PM}}^2[dm(t)/dt]^2$ can be neglected, which is verified by the experiment. The ac term of the photocurrent after the PD is

$$i_{\mathrm{sig}}(t) = 2\Re K^2(\omega_c - \omega_0)\beta_{\mathrm{PM}}\frac{dm(t)}{dt}. \tag{6}$$

From (6), it is clearly seen that the detected signal after the PD is proportional to the first-order derivative of the applied modulating signal. Therefore, if the PM signal $m(t)$ is a Gaussian pulse, after the linear frequency discriminator, a Gaussian monocycle is generated, as shown in Fig. 2. In addition, it can be seen from (6) that the sign of $i_{\mathrm{sig}}(t)$ is determined by $(\omega_c - \omega_0)$ and β_{PM}. If the PM index β_{PM} is fixed, the sign of $(\omega_c - \omega_0)$ determines the sign of $i_{\mathrm{sig}}(t)$. For $\beta_{\mathrm{PM}} > 0$, if $(\omega_c - \omega_0) > 0$, $i_{\mathrm{sig}}(t)$ has the same polarity as $dm(t)/dt$, while if $(\omega_c - \omega_0) < 0$, an inverted pulse $-(dm(t)/dt)$ is obtained. Therefore, by locating the optical carrier ω_c at the different slopes of the optical bandpass filter, the UWB monocycle pulses with inverted polarities can be generated, as shown in Fig. 2. This analytical result is consistent with our earlier experimental results in [15], where an FBG was used to serve as a frequency discriminator. Gaussian monocycle pulses with inverted polarities were experimentally generated by locating the optical carrier at the left and right slopes of the FBG.

On the other hand, the polarity of a monocycle can also be switched by rotating the polarization direction of the incident light. If the optical carrier is fixed at one slope of the optical bandpass filter, the sign of $(\omega_c - \omega_0)$ would be fixed. Since the PM indexes along the TE and TM directions in the PolM are opposite, that is, $\beta_{\mathrm{PM}}(\mathrm{TE}) = -\beta_{\mathrm{PM}}(\mathrm{TM})$, the Gaussian monocycles generated along the TE and TM directions would be complementary. Therefore, by rotating the polarization direction of the incident lightwave along the TE or the TM direction, a UWB monocycle with switchable polarity

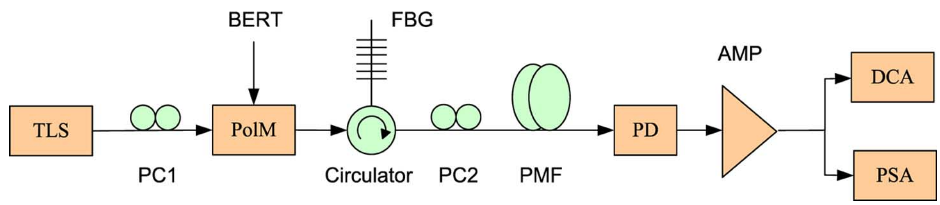

Fig. 3. Experiment setup of the proposed switchable UWB pulse generator.

is generated. This property is very important, since the system can implement the PPM scheme by simply adjusting the voltage applied to AWP_1. In addition, the system here is much simpler compared to the approach demonstrated in [15], where the PPM scheme was implemented by switching the optical wavelength. Furthermore, the speed of the proposed system is much faster, since a state-of-the-art AWP can operate at a speed up to 40 Gb/s [17].

C. UWB Doublet Generation

The proposed system shown in Fig. 1 can also be used to generate UWB doublet pulses. To do so, the voltage applied to the AWP_1 is adjusted such that the incident lightwave to the PolM is circularly polarized. It is known that a circularly polarized lightwave can be considered as two linearly polarized lightwaves along the TE and TM directions with a phase difference of 90°. If the TE and TM modes are traveling in the PolM, they will experience PM but with opposite PM indexes. After frequency discrimination, two complementary monocycle pulses are obtained. If the two monocycle pulses are directly detected by a PD, no signal will be generated due to the cancellation of the two complementary pulses. However, if a length of PMF is incorporated between the PolM and the PD, by aligning the TE and TM modes with the two principal axes of the PMF, a time-delay difference would be introduced due to the birefringence of the PMF. The whole system is now equivalent to a two-tap microwave delay-line filter with coefficients of $(1\ -1)$. It is known that the frequency response of a two-tap delay-line filter is

$$H_{\text{Two-Tap}}(\omega) = 1 - e^{-j\omega\tau} = 2j\sin\frac{\omega\tau}{2}e^{-\frac{j\omega\tau}{2}} \quad (7)$$

where $H_{\text{Two-Tap}}(\omega)$ is the frequency response, and τ is the time-delay difference.

If $\omega\tau/2$ is small, (7) can be approximated as

$$H_{\text{Two-Tap}}(\omega) = j\omega\tau e^{-\frac{j\omega\tau}{2}}. \quad (8)$$

As can be seen, (8) has the same frequency response as a first-order differentiator except that a scaling factor and a linear phase shift are added, which will not affect the shape of the output signal. As we have discussed earlier, the first-order derivative of a Gaussian monocycle is a Gaussian doublet, which can be approximated by a first-order difference. Therefore, if a UWB monocycle is inputted in the two-tap delay-line filter, a UWB doublet pulse would be generated.

The polarity of the generated doublet pulse can also be switched. To do so, we need to incorporate a second AWP, i.e., AWP_2 shown in Fig. 1, to rotate the polarization directions of the TE and TM modes after the PolM by a 90°. After the rotation, the TM mode will travel with a longer optical distance than that of TE mode. The frequency response of the two-tap delay-line filter is now given as

$$H_{\text{Two-Tap}}(\omega) = -1 + e^{-j\omega\tau} = -j\omega\tau e^{-\frac{j\omega\tau}{2}}. \quad (9)$$

Comparing (8) and (9), it is clearly seen that the generated pulse is an inverted version of the one without the polarization rotation. Again, the speed of the system here is much faster than the approach in [15], since a state-of-the-art AWP can operate at a speed up to 40 Gb/s.

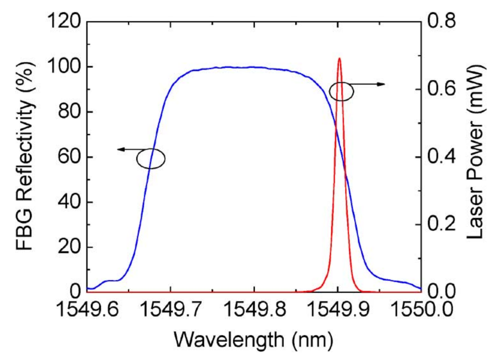

Fig. 4. Reflection spectrum of the FBG. The optical carrier is tuned to locate at the right slope of the FBG spectrum.

III. Experimental Results and Discussions

The proposed UWB pulse generator is experimentally demonstrated. The experimental setup is shown in Fig. 3. A tunable laser source (TLS) with an output power of 10 mW is used to generate the incident lightwave. An FBG is used to serve as the frequency discriminator. The FBG is fabricated in a hydrogen-loaded fiber using a frequency-doubled ion argon laser operating at 244 nm with a phase mask. The center wavelength of the FBG is 1549.79 nm, and the reflectivity is greater than 99%. To suppress the sidelobes, a Gaussian apodization profile is incorporated during the FBG fabrication process. The FBG has a sidelobe suppression ratio better than 13 dB. In the experiment, the wavelength of the TLS is tuned at 1549.9 nm to make the optical carrier locate at the right slope of the FBG reflection spectrum, as shown in Fig. 4. The PolM (Versawave Technologies) used in the experiment can operate up to 40 GHz with a wavelength range from 1530 to 1560 nm. The PMF (Corning PM1550) has a beat length of 3.75 mm, and 42 m of the PMF provides a time-delay difference of about

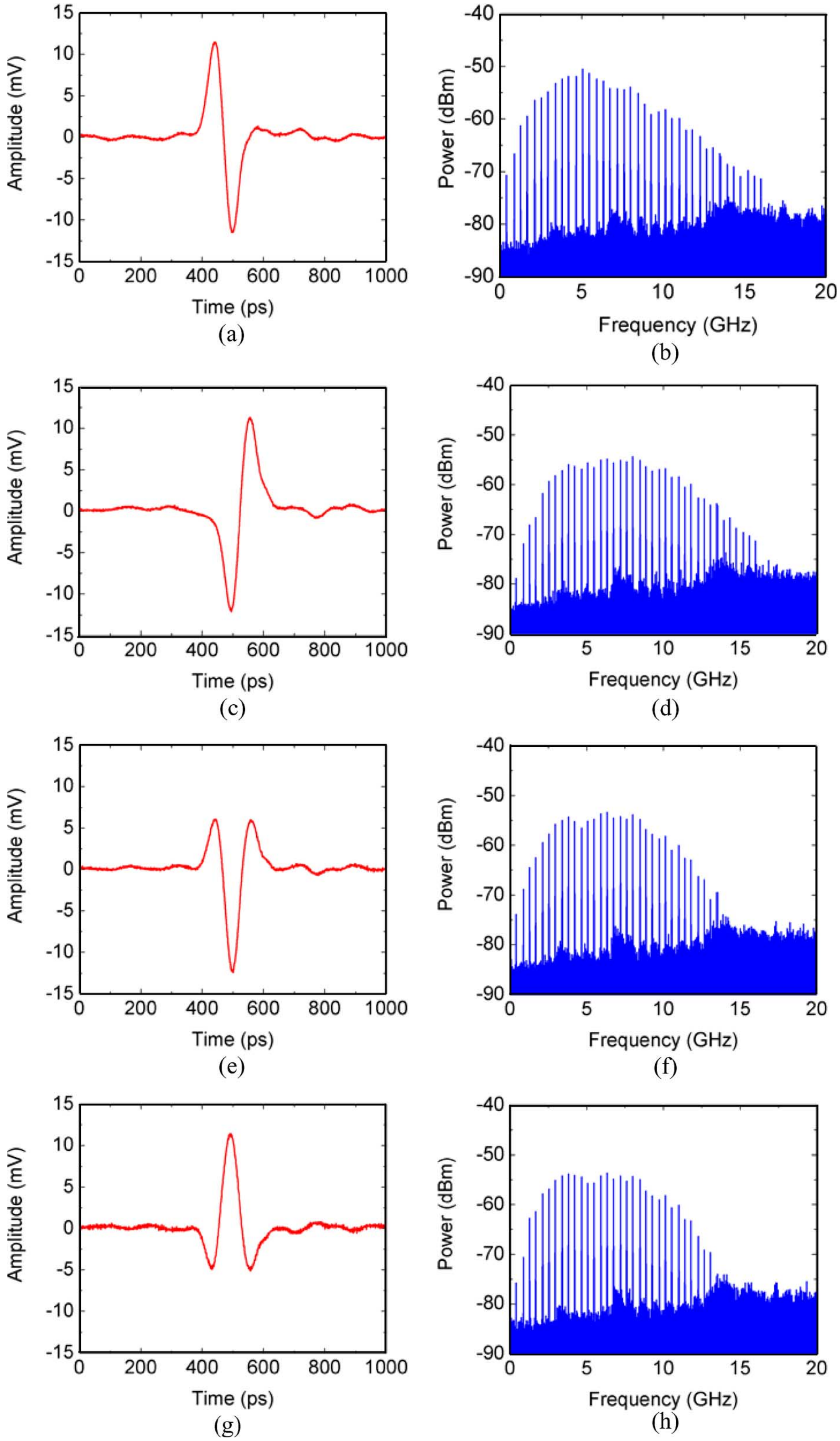

Fig. 5. Waveforms and spectra of the UWB Gaussian monocycle and doublet pulses generated in the experiment. Left column: Waveform. Right column: Spectrum. (a)–(d) Monocycles. (e)–(h) Doublets.

57 ps. A data sequence generated by a bit-error-rate tester (BERT) (Agilent N4901B) is applied to the PolM. The data sequence has a data rate of 13.5 Gbit/s with a fixed pattern of one "1" and 31 "0." The shape of the modulation signal is close to a Gaussian pulse with a full-width at half-maximum of about 63 ps. Since no AWPs are available at the time of the experiment, two polarization controllers (PCs) are used to replace AWP_1 and AWP_2. The generated UWB pulses are monitored by a high-speed oscilloscope (DCA, Agilent 86100C) and a power spectrum analyzer (PSA, Agilent E4448A).

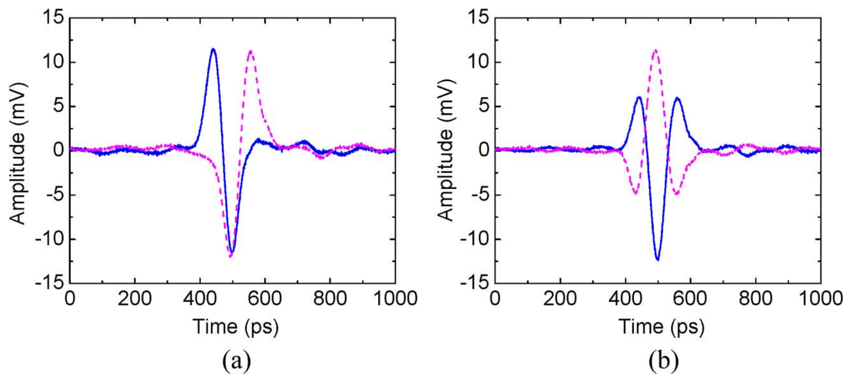

Fig. 6. Temporal relationship between the polarity-switched pulses. (a) Polarity-inverted monocycle pulses. (b) Polarity-inverted doublet pulses.

In the experiment, we adjust PC1 to align the polarization direction of the TLS output with one principal axis (e.g., x-axis) of the PolM, and adjust PC2 to align the x-axis of the PolM with the fast axis of the PMF. When a Gaussian pulse is applied to the PolM, a Gaussian monocycle pulse is generated. The waveform and the spectrum of the generated UWB monocycle pulse are shown in Fig. 5(a) and (b). To demonstrate the switchability of the generated pulses, we fix PC2 and adjust PC1. Once the lightwave from the TLS is rotated by 90° (aligned with the y-axis), a polarity-inverted monocycle is generated, as shown in Fig. 5(c), with its spectrum shown in Fig. 5(d). The pulse switchability for the UWB monocycle pulses is demonstrated.

When the polarization state of the lightwave from the TLS is adjusted by PC1 to be circularly polarized, a UWB doublet pulse is generated, as shown in Fig. 5(e). The spectrum of the UWB doublet pulse is shown in Fig. 5(f). As we have discussed earlier, the polarity of the UWB doublet pulse can also be switched. To do so, we adjust PC2 to rotate the polarization directions of the TE and TM modes at the output of the PolM by 90°, a polarity-inverted UWB doublet is generated, as shown in Fig. 5(g), with its spectrum shown in Fig. 5(h). The -10 dB bandwidths of the generated UWB monocycle and the doublet pulses are measured to be about 9.3 and 10.5 GHz, with fractional bandwidths of 150% and 160%, respectively. The stability of the generated UWB monocycle and doublet pulses is mainly affected by the wavelength drifts of the TLS and the FBG. Since the TLS is precisely temperature controlled, its effect is minimized. For the FBG, the effect is negligible if the wavelength drift of the FBG can be controlled to maintain the optical carrier within the linear region of the FBG spectrum slope. In the experiment, a stable UWB pulse generation is observed at room temperature.

The temporal relationship between the polarity-switched pulses is also studied. In Fig. 6(a), two polarity-inverted UWB monocycle pulses are shown. It is clearly seen that there is a time shift between the two polarity-inverted monocycle pulses. The time shift is equal to the time-delay difference between the TE and the TM modes traveling in the PMF, since the two monocycle pulses are generated when the TE and TM modes are traveling along the fast and slow axes of the PMF. The time shift is measured to be about 55 ps, which is close to the time-delay difference of 57 ps calculated based on the birefringence and the length of the PMF. This time shift may not be wanted in a UWB communication system that employs PPM scheme. A possible solution is to synchronize the control voltages applied to AWP_1 and AWP_2 to rotate the polarization directions of the lightwave entering and exiting the PolM simultaneously, which will make the two complementary UWB monocycle pulses travel along the same principle axis of the PMF.

The time shift problem is not observed for the UWB doublet pulses, as shown in Fig. 6(b). This is also clearly seen from (7) and (8). The UWB doublet pulse in (7) is exactly the pulse in (8), except that the pulse in (8) is an inverted version of the pulse in (7) (a negative sign in the equation).

We should note that by controlling the voltages applied to the AWPs, the shape of the generated UWB pulses can also be switched, from a monocycle to a doublet, or vice versa. This property makes the PSM scheme possible.

In the experiment, the two AWPs are replaced by two PCs. For practical applications, high-speed electrically switchable AWPs must be employed to meet the high-speed modulation requirement. Generally, the two AWPs can be two additional PolMs, since a PolM is generally an AWP that can operate at a high speed. In addition, the three PolMs can be fabricated on a single chip to ensure an excellent polarization alignment and make the whole system compact and have a better stability.

In obtaining (8), we assume that $\omega\tau/2$ is small; therefore, the first-order derivative can be well approximated by a first-order difference, which could be implemented using the two-tap microwave delay-line filter. If τ is not very small, the shape of the generated doublet will be distorted. A simulation is performed to show an ideal doublet and a doublet generated by using a microwave delay-line filter with coefficients of $(1\ -1)$ with different τ in Fig. 7. The Gaussian pulse used in the simulation is $G(t) = \exp(-t^2/50^2)$, and the corresponding Gaussian monocycle is $G'(t) = -(2t/50^2)\exp(-t^2/50^2)$. As can be seen when the time-delay difference is 60 ps, the difference between an ideal doublet and the generated waveform is very small. In our experiment, the time-delay difference is set at 57 ps. Therefore, the generated doublet can be considered to be an ideal UWB doublet.

IV. Conclusion

An electrically switchable optical UWB pulse generator that was capable of generating polarity-inverted Gaussian

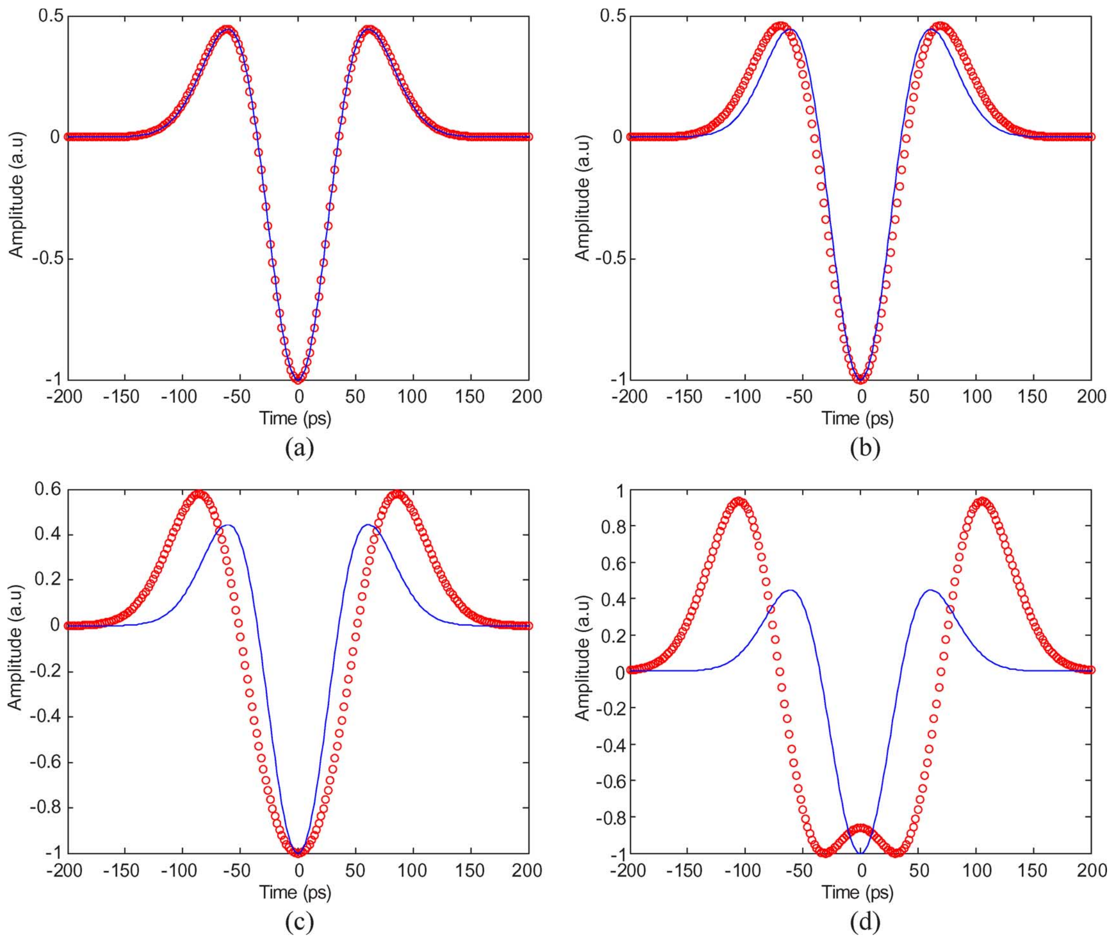

Fig. 7. Comparison of an ideal doublet and a doublet generated by using a microwave delay-line filter. Solid line: Ideal doublet. Circles: Doublet generated using the microwave delay-line filter. (a) $\tau = 20$ ps. (b) $\tau = 60$ ps. (c) $\tau = 100$ ps. (d) $\tau = 140$ ps.

monocycle and doublet pulses using a PolM and an FBG was proposed and experimentally demonstrated. The key component in the system is the PolM, which is a special phase modulator that supports both TE and TM modes, with opposite PM indexes for the TE and TM modes. The key advantage of the proposed UWB pulse generator is that it can generate either the UWB monocycle or doublet pulses in a single system by simply adjusting the voltages applied to the AWPs. An added advantage of the proposed system is that by controlling the voltages applied to the AWPs, the polarity and the shape of the UWB pulses can also be switched. For high-speed communications, the switching speed should be high, which can be realized by using high-speed electrically controlled AWPs. Usually, a PolM can function as an electrically controlled AWP. Therefore, the proposed generator can be implemented using three PolMs, with the PolMs integrated on a single chip. The proposed UWB pulse generator would find applications in the UWB communications and radar systems employing PPM or PSM schemes.

REFERENCES

[1] D. Porcine, P. Research, and W. Hirt, "Ultra-wideband radio technology: Potential and challenges ahead," *IEEE Commun. Mag.*, vol. 41, no. 7, pp. 66–74, Jul. 2003.

[2] G. R. Aiello and G. D. Rogerson, "Ultra-wideband wireless systems," *IEEE Microw. Mag.*, vol. 4, no. 2, pp. 36–47, Jun. 2003.

[3] R. J. Fontana, "Recent system applications of short-pulse ultra-wideband (UWB) technology," *IEEE Trans. Microw. Theory Tech.*, vol. 52, no. 9, pp. 2087–2104, Sep. 2004.

[4] M. Ghavami, L. B. Michael, and R. Kohno, *Ultra-Wideband Signals and Systems in Communication Engineering*. Hoboken, NJ: Wiley, 2004.

[5] K. Siwiak and D. Mckeown, *Ultra-Wideband Radio Technology*. Hoboken, NJ: Wiley, 2004.

[6] J. Han and C. Nguyen, "New ultra-wideband, ultra-short monocycle pulse generator with reduced ringing," *IEEE Microw. Wireless Compon. Lett.*, vol. 12, no. 6, pp. 206–208, Jun. 2002.

[7] J. S. Lee, C. Nguyen, and T. Scullion, "New uniplanar subnanosecond monocycle pulse generator and transformer for time-domain microwave applications," *IEEE Trans. Microw. Theory Tech.*, vol. 49, no. 6, pp. 1126–1129, Jun. 2001.

[8] W. P. Lin and J. Y. Chen, "Implementation of a new ultrawide-band impulse system," *IEEE Photon. Technol. Lett.*, vol. 17, no. 11, pp. 2418–2420, Nov. 2005.

[9] L. Zhu, S. Sun, and W. Menzel, "Ultra-wideband (UWB) bandpass filters using multiple-mode resonator," *IEEE Microw. Wireless Compon. Lett.*, vol. 15, no. 11, pp. 796–798, Nov. 2005.

[10] T. Kawanishi, T. Sakamoto, and M. Izutsu, "Ultra-wide-band signal generation using high-speed optical frequency-shift-keying technique," in *IEEE Int. Top. Meeting MWP Tech. Dig.*, Oct. 2004, pp. 48–51.

[11] Q. Wang and J. P. Yao, "UWB doublet generation using a nonlinearly-biased electro-optic intensity modulator," *Electron. Lett.*, vol. 42, no. 22, pp. 1304–1305, Oct. 2006.

[12] Q. Wang, F. Zeng, S. Blais, and J. P. Yao, "Optical UWB monocycle pulse generation based on cross-gain modulation in a semiconductor optical amplifier," *Opt. Lett.*, vol. 31, no. 21, pp. 3083–3085, Nov. 2006.

[13] C. Wang, F. Zeng, and J. P. Yao, "All-fiber ultrawideband pulse generation based on spectral shaping and dispersion-induced frequency-to-time

conversion," *IEEE Photon. Technol. Lett.*, vol. 19, no. 3, pp. 137–139, Feb. 2007.

[14] I. S. Lin, J. D. McKinney, and A. M. Weiner, "Photonic synthesis of broadband microwave arbitrary waveforms applicable to ultra-wideband communication," *IEEE Microw. Wireless Compon. Lett.*, vol. 15, no. 4, pp. 226–228, Apr. 2005.

[15] F. Zeng and J. P. Yao, "Ultrawideband impulse radio signal generation using a high-speed electrooptic phase modulator and a fiber-Bragg-grating-based frequency discriminator," *IEEE Photon. Technol. Lett.*, vol. 18, no. 19, pp. 2062–2064, Oct. 2006.

[16] F. Zeng and J. P. Yao, "An approach to ultrawideband pulse generation and distribution over optical fiber," *IEEE Photon. Technol. Lett.*, vol. 18, no. 7, pp. 823–825, Apr. 2006.

[17] J. D. Bull, N. A. F. Jaeger, H. Kato, M. Fairburn, A. Reid, and P. Ghanipour, "40 GHz electro-optic polarization modulator for fiber optic communications systems," *Proc. SPIE*, vol. 5577, no. 1, pp. 133–143, Sep. 2004.

[18] J. P. Yao, F. Zeng, and Q. Wang, "Photonic generation of ultra-wideband signals," *J. Lightw. Technol.*, vol. 25, no. 11, Nov. 2007.

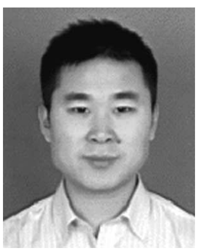

Qing Wang received the B.Sc. and Ph.D. degrees in electronic engineering from Tsinghua University, Beijing, China, in 2000 and 2006, respectively.

Since March 2006, he has been a Postdoctoral Research Fellow with the Microwave Photonics Research Laboratory, School of Information Technology and Engineering, University of Ottawa, Ottawa, ON, Canada. His research interests include fiber amplifiers and lasers, fiber Bragg gratings, nonlinearities in fiber- and semiconductor-based optical devices, and photonic generation and processing of microwave signals.

Jianping Yao (M'99–SM'01) received the Ph.D. degree in electrical engineering from the Université de Toulon, Toulon, France, in 1997.

In 2001, he joined the School of Information Technology and Engineering, University of Ottawa, Ontario, ON, Canada, where he is currently a Professor, the Director of Microwave Photonics Research Laboratory, and the Director of Ottawa-Carleton Institute for Electrical and Computer Engineering. From 1999 to 2001, he was a faculty member with the School of Electrical and Electronic Engineering, Nanyang Technological University, Singapore. He has been a Guest Professor at Shantou University, Shantou, China, and Sichuan University, Chengdu, China. He spent three months as an Invited Professor with the Institut National Polytechnique de Grenoble, Grenoble, France, in 2005. He has published over 160 papers in refereed journals and conference proceedings. His research interests include microwave photonics, which includes all-optical microwave signal processing, photonic generation of microwaves, millimeter-wave and terahertz, radio over fiber, UWB over fiber, fiber Bragg gratings for microwave photonics applications, optically controlled phased array antennas, fiber lasers, fiber-optic sensors, and bio-photonics.

Dr. Yao is a Registered Professional Engineer in Ontario. He is a member of the International Society for Optical Engineers and of the Optical Society of America. He is a Senior Member of the IEEE Lasers and Electro-Optics Society and the IEEE Microwave Theory and Techniques Society.